International Journal of Minerals, Metallurgy and Materials
Volume 22, Number 4, April 2015, Page 411
DOI: 10.1007/s12613-015-1087-x

Microstructure and texture evolution of Mg–3Zn–1Al magnesium alloy during large-strain electroplastic rolling

Yan-bin Jiang[1)], *Lei Guan*[2)], *Guo-yi Tang*[3)], *Bo Cheng*[2)], *and Da-bo Liu*[2)]

1) Key Laboratory for Advanced Materials Processing of the Ministry of Education, Institute of Advanced Materials and Technology, University of Science and Technology Beijing, Beijing 100083, China

2) Beijing Institute of Aeronautical Materials, Aviation Industry Corporation of China, Beijing 100095, China

3) Advanced Materials Institute, Graduate School at Shenzhen, Tsinghua University, Shenzhen 518055, China

(Received: 27 June 2014; revised: 15 September 2014; accepted: 15 September 2014)

Abstract: Large-strain deformation by single electroplastic rolling (EPR) was imposed on AZ31 magnesium alloy strips. During EPR at low temperature (150–250°C), numerous twins formed in the alloy. After EPR at a high temperature (350°C), the number of twins reduced and some dynamic recrystallization (DRX) grains formed at grain boundaries and twinned regions. The synergic thermal and athermal effects generated by electropulsing, which promoted dislocation motion, induced a few small DRX grains, and ductile bandings were mainly responsible for large-strain deformation during EPR. The inclination angle of the basal pole stemmed from the counterbalance of the inclination direction of the basal pole between the DRX grains and deformed coarse grains.

Keywords: magnesium alloys; electroplastic rolling; microstructure; texture; recrystallization

1. Introduction

Wrought magnesium alloys have great potential as lightweight structural materials, particularly in some automotive and electronic applications, because of their excellent properties, which include low density, high specific strength, and good damping capacity [1]. However, their widespread application is limited by their poor formability at low temperatures, which is due to their hexagonal crystal structure with few independent slip systems. Grain refinement [2–5] and texture modification [6–10] are effective methods to substantially improve the ductility and formability of wrought magnesium alloys. Grain refinement can be achieved in Mg alloys through adoption of the novel technology of electropulsing treatment (EPT) [11–16], and the results of our previous study [13] indicated that the recrystallized grains give rise to a tilted basal texture during EPT, which is favorable for enhancing the ductility and formability of Mg–3Al–1Zn (AZ31) alloy. Grain refinement can also be achieved through large strain rolling (LSR) [17]. LSR has some advantages that stem from its simplicity and greater ability to form large parts (sheets) compared to other processing methods of severe plastic deformation (SPD) [18], such as equal channel extrusion (ECAE), accumulative roll bonding (ARB), or high-pressure torsion (HPT). Therefore, LSR is considered as one of the most promising methods for the industrial production of magnesium alloys. However, LSR at room temperature is not possible, especially in the case of rolling of thin AZ31 alloy strips. Because magnesium alloys exhibit a severe work-hardening effect, after accumulated cold rolling reduction exceeds approximately 25%, intermediate annealing is required for subsequent rolling, which results in a series of problems, including a long process flow, high energy consumption, and high production costs. An increase in the rolling temperature (300–400°C) can enhance the ductility and formation by activating non-basal slip systems [19]; however, inevitable problems with the thickness tolerance and the shape of the resulting strip are difficult to overcome due to the high tem-

Corresponding author: Lei Guan E-mail: guanlei06@tsinghua.org.cn

perature.

Our study indicated that electroplastic rolling (EPR) functions as a novel technology for improving the formability of the AZ31 alloy by activating a non-basal slip system and inducing dynamic recrystallization [20]. Large-strain deformation by EPR is important for extending the engineering applications of EPR to the production of magnesium alloy strips or sheets. In the present work, large-strain deformation by single EPR was conducted on AZ31 strips and the microstructure, texture development, and mechanical properties of the AZ31 strip during EPR were investigated.

2. Experimental

AZ31 magnesium alloy (3.1wt% Al, 0.9wt% Zn, 0.2wt% Mn, and balance Mg) ingots were extruded into strips with a thickness of 1.5 mm. The extruded strips were annealed at 300°C for 1 h. The as-annealed strips were electroplastic-rolled to a thickness of 1.05 mm by a single pass of 30% reduction. The rolling direction (RD) was parallel to the extrusion direction (ED). The EPR process is schematically illustrated in Fig. 1. The AZ31 strip was rolled under multiple electropulsing while moving at a speed of 2 m/min over a distance of 225 mm between the two electrodes. A custom-made electropulsing generator was used to supply the positive multiple pulses, and electropulses with various frequencies and durations (70–80 μs) were applied to the strip. The electrical parameters, including the frequency, root-mean-square (RMS) current, discharge voltage, amplitude, and duration of the current pulses were monitored by a Hall-effect sensor connected to an oscilloscope. During EPR, the temperature of the AZ31 strip increased with increasing distance from the anode because of accumulation of the Joule heating effect. The temperature at the entrance of the roller, which was measured using a Raytek MX2 infrared thermoscope, approached a maximum. To rule out a hysteresis effect of the thermoscope on the temperature measurements, each measured temperature was taken to be valid when the value recorded was relatively steady. The Raytek MX2 infrared thermoscope was repeatedly calibrated using a thermocouple prior to each temperature measurement. The EPR parameters of the strips are listed in Table 1.

X-ray texture analysis was conducted on the surface of the as-annealed and EPR samples. Five incomplete pole figures (up to $\psi = 70°$), (0002), $(10\bar{1}0)$, $(10\bar{1}1)$, $(10\bar{1}2)$, and $(\bar{2}110)$ were acquired from each sample by X-ray diffraction in the back-reflection mode using Co K_α radiation. The pole figures showed that only the (0002) basal plane texture was developed; therefore, only the (0002) pole figure is presented in this paper. Prior to being optically examined, the samples were sectioned, cold mounted, and polished with 6- and 1-μm diamond paste. They were then etched in acetic picral (5 mL of acetic acid, 6 g of picric acid, 35 mL of ethanol, and 5 mL of water) for 5 s. The average grain size was calculated from the optical micrographs using the linear intercept method. Uniaxial tensile tests were conducted at room temperature at a rate of 0.5 mm/min over a gauge length of 50 mm. The tensile axis was parallel to the rolling direction. Five samples prepared under each set of conditions listed in Table 1 were tested.

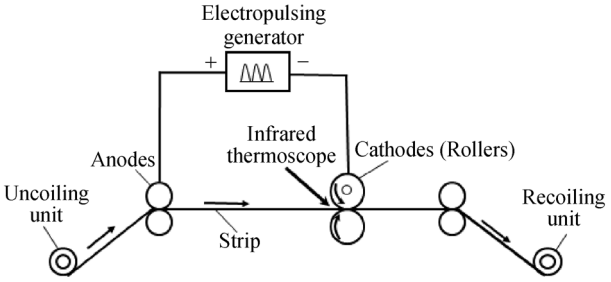

Fig. 1. Schematic of the EPR process.

Table 1. Experimental conditions of AZ31 Mg alloy under EPR

EPR Sample No.	Frequency / Hz	Discharge voltage / V	J_m / (A·mm^{-2})	J_e / (A·mm^{-2})	Temperature / °C
1	131	6.24	282.99	425	150
2	131	7.20	362.53	490	200
3	131	8.08	366.44	547	250
4	131	8.48	384.58	568	300
5	131	8.98	407.26	598	350

Note: J_m is the amplitude of current density of electropulsing, and J_e represents the RMS value of current density during EPR and is related to the Joule heating effect.

3. Results

The microstructure and texture of the as-annealed AZ31 alloy are shown in Fig. 2. The optical micrographs show equiaxed grains with an average grain size of approximately 50 μm formed in the as-annealed AZ31 alloy. The texture is shown in Fig. 2(c) by means of the (0002) pole figure. As evident in the figure, a strong basal fiber texture was formed in the AZ31 alloy. A large volume fraction of grains was oriented on the basal planes parallel to the rolling plane.

Fig. 3(a) shows the relationship between the hardness and temperature of the EPR samples. As the entrance temperature was increased, the hardness first increased and then decreased. When the temperature was increased from 150°C to

250°C, the hardness increased to its maximum value. As the temperature was raised further, the hardness decreased. The curve can be divided into two regions: the hardening stage (150–250°C) and the softening stage (250–350°C). Fig. 3(b) illustrates the dependences of tensile strength and elongation to failure on temperature. The tensile strength of the EPR samples increased during the hardening stage and decreased during the softening stage. However, the elongation to failure increased to 12%–14.5% when the temperature exceeded 200°C .

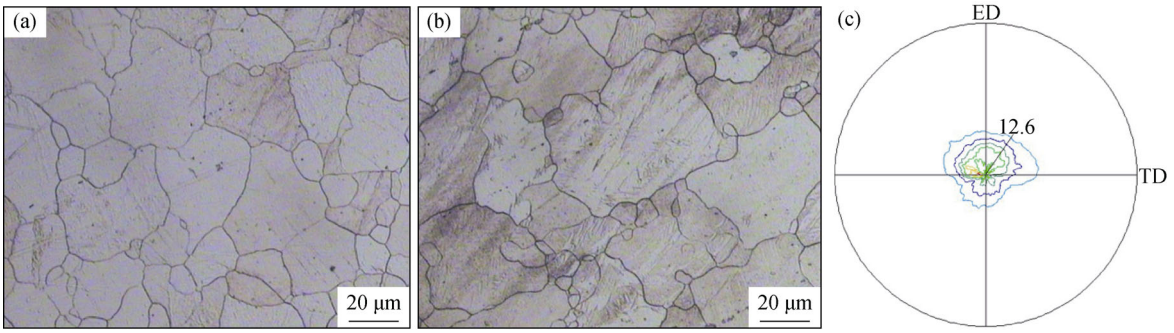

Fig. 2. Microstructures of the as-annealed AZ31 alloy: (a) ED–TD plane; (b) ED–ND plane; (c) (0002) pole figure.

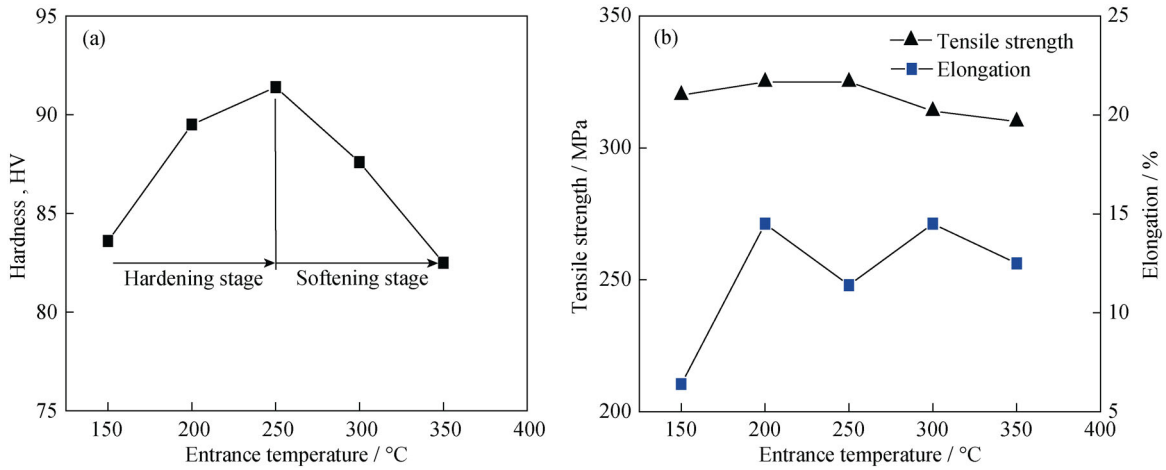

Fig. 3. Mechanical properties of the EPR samples: (a) relationship between hardness and entrance temperature; (b) relationships of tensile strength and elongation to entrance temperature.

The microstructures of the EPR1, EPR3, and EPR5 samples are shown in Figs. 4(a)–4(f). The micrographs were taken in the middle of the samples along the rolling plane (RP) (Figs. 4(a)–4(c)) and along the plane formed by the rolling direction (RD) and normal direction (ND) (i.e., the RN plane) (Figs. 4(d)–4(f)). As evident in Figs. 4(a)–4(f), no significant grain refinement occurred after EPR, and extensive twinning occurred in the original grains. In the hardening stage, when the temperature increased, the volume fraction of the twinned materials increased significantly and the extent to which the deformed coarse grains were broken up also increased, as shown in Figs. 4(d) and 4(e). During the softening stage, as the temperature was increased, the number of shear bands and twins diminished, as shown in Figs. 4(b) and 4(c). The extent of break-up was remarkably reduced, and prolonged coarse grains along the RD were apparent, as shown in Figs. 4(e) and 4(f). Notably, new small DRX grains formed at the grain boundaries and twinned regions ("mantle") during EPR. The mantle region became thicker during the hardening stage and thinner during the softening stage. Figs. 4(g)–4(h) illustrate the texture of the EPR samples by means of the (0002) pole figures. The *c*-axis of the EPR samples was inclined approximately 5°–15° from the ND toward the RD, with slightly weakened basal texture intensity compared to that of the as-annealed sample. A double peak obviously appeared in the pole figure of sample EPR3, as shown in Fig. 4(h).

4. Discussion

During EPR in this work, the temperature gradient between the cold rollers and the hot sample caused heat loss of

the sample via conduction. According to the theory of thermal equilibrium and neglecting heat loss via convection and radiation between air and the hot sample, the net conductive heat transfer per unit between the rollers and sample can be described by the following relationship:

$$2\lambda S(T_1 - T_2)/\delta = C\rho H_m B v \Delta T \quad (1)$$

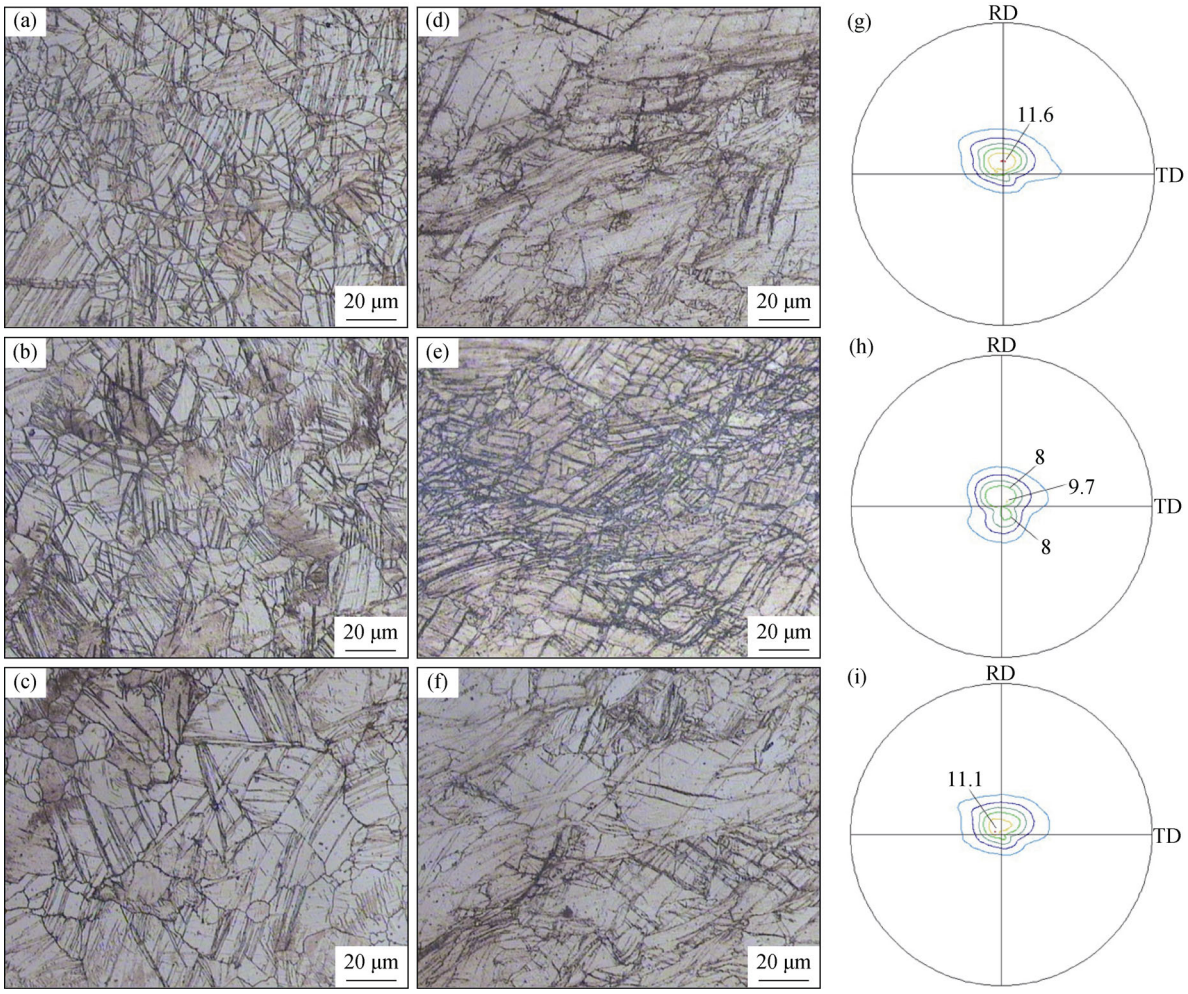

Fig. 4. Microstructure and macrotexture of the EPR samples: (a) RP, EPR1; (b) RP, EPR3; (c) RP, EPR5; (d) RN plane, EPR1; (e) RN plane, EPR3; (f) RN plane, EPR5; (g) (0002) pole figure, EPR1; (h) (0002) pole figure, EPR3; (i) (0002) pole figure, EPR5.

where T_1 is the temperature of the sample, T_2 is the temperature of rollers, λ is the thermal conductivity of the magnesium alloy, S is the contact area between the roller and sample, δ is the thickness of the oxide layer on the sample, C is the specific heat capacity of the magnesium alloy, ρ is the density of the magnesium alloy, H_m is the mean height of the sample, B is the breadth of the rolled sample at the exit, v is the rolling velocity, and ΔT is the temperature decrement of the sample. The temperature decrement ΔT can be obtained according to Eq. (1):

$$\Delta T = \frac{2\lambda l}{C\rho H_m v}(T_1 - T_2) \quad (2)$$

where l is the length of the deformed arc of the contact region due to roll flattening.

According to Eq. (2), the temperature decrement of the sample increases with increasing entrance temperature. We expected that, under the experimental conditions used in this investigation, the temperature decrement of the sample would reach the maximum when the entrance temperature was 250°C, which was demonstrated when the exit temperature of the EPR3 sample was at its minimum in our experiment. Such behavior induced the hardening stage when the entrance temperature was increased from 150°C to 250°C. At higher entrance temperatures (250–350°C), the effect of heat loss was diminished, which gave rise to the softening stage. After EPR, no significant grain refinement arose from the substantial heat loss between the cold rollers and the hot sample, thereby resulting in a slight change in the tensile strength with respect to the Hall–Petch relationship. The large amount of twinned coarse grains resulted in

the low elongation to failure of the EPR samples.

In general, both basal-plane slip and twining are the deformation mechanisms of the AZ31 alloy during rolling, which commonly resulted in numerous twins inside grains and the strong basal texture [13]. The workability per pass rolling of the AZ31 alloy is limited by its lack of deformation models. Enhancing the plastic deformation model is an effective method for improving the workability of Mg alloys. EPR can effectively activate a non-basal slip system and promote dislocation motion and interactions based on the combined thermal and athermal effects arising from electropulsing [11,13,20]. The combined thermal and athermal effects increased substantially as the discharge voltage and the temperature were increased. In this work, the heat loss caused by conduction between the cold rollers and the hot samples strongly affected the samples' microstructure and texture evolution. During the hardening stage (150–250°C), as the heat loss effect increased, the combined thermal and athermal effects were limited and dislocation motion could not be substantially activated. The contribution of twinning to the plastic deformation was enhanced, and the extent to which the deformed coarse grains were broken up increased. In the softening stage (250–350°C), as the heat loss effect weakened and the deformation temperature increased, the combined thermal and athermal effects increased remarkably. These increased thermal and athermal effects promoted the dislocation motion, which partially compensated for the contribution of twinning to plastic deformation, as demonstrated by the remarkable reduction in the number of twins, the elongation of coarse grains along the RD, and the reduction in the extent of break-up (Figs. 4(c) and 4(f)). Additionally, the increase of the combined thermal and athermal effects resulted in the formation of new small recrystallized grains at the grain boundaries and twinned regions. When the new DRX grains were formed, they tended to cluster in large banded areas, with an orientation that favored the development of basal slip, commonly called "ductile bandings". Deformation then concentrated in these regions, and basal slip became the main deformation mechanism to accommodate the greater strain. Therefore, a single large-strain deformation of AZ31 alloy can be achieved by EPR at low temperatures.

In the magnesium alloys, the dynamic recrystallization (DRX) mechanism strongly depends on the initial texture. Rotational dynamic recrystallization (RDRX) has been reported to occur in extruded AZ61 plates with an initial strong basal texture [17]. During EPR, the large reduction per pass introduced large stress concentration around the grain boundaries of the coarse grains with an unfavorable orientation for basal slip, thereby prompting RDRX. Within the ductile bandings, however, the new small DRX grains were rotated away from the original coarse grains mostly belonging to the {0001} fiber, which weakened the basal texture. Therefore, we concluded that the small inclination angles of the *c*-axis were due to the counterbalance from the opposite effect on the inclination direction of the basal pole between the ductile bandings and the coarse-grain regions.

5. Conclusion

During large-strain EPR, two stages of hardening and softening occurred as the entrance temperature was increased. Heat loss between the cold rollers and the hot sample occurred mainly via conduction, and no significant grain refinement occurred after EPR. Under the combined thermal and athermal effects, new small DRX grains formed at the grain boundaries and at the twinned regions consisting of ductile bandings. The synergic thermal and athermal effects generated by electropulsing, which promoted dislocation motion, induced a few small DRX grains; in addition, ductile bandings were mainly responsible for large-strain deformation during EPR. The small inclination angles of the *c*-axis stemmed from the counterbalance in the inclination direction of the basal pole between the ductile bandings and the coarse-grain regions.

Acknowledgements

The authors would like to thank the support from the National Natural Science Foundation of China (Nos. 51104016 and 50571048), the National High Technology Research and Development Program of China (No. 2013AA031301), and the fund of the State Key Laboratory of Advanced Technologies for Comprehensive Utilization of Platinum Metals (No. SKL–SPM–201204).

References

[1] B.L. Mordike and T. Ebert, Magnesium: properties–applications–potential, *Mater. Sci. Eng. A*, 302(2001), No. 1, p. 37.

[2] Y. Chino and M. Mabuchi, Influences of grain size on mechanical properties of extruded AZ91 Mg alloy after different extrusion processes, *Adv. Eng. Mater*., 3(2001), No. 12, p.

981.

[3] T. Mukai, M. Yamanoi, H. Watanabe, and K. Higashi, Ductility enhancement in AZ31 magnesium alloy by controlling its grain structure, *Scripta Mater*., *4*5(2001), No. 1, p. 89.

[4] J. Koike, T. Kobayashi, T. Mukai, H. Watanabe, M. Suzuki, K. Maruyama, and K. Higashi, The activity of non-basal slip systems and dynamic recovery at room temperature in fine-grained AZ31B magnesium alloys, *Acta Mater*., 51(2003), No. 7, p. 2055.

[5] J. Koike, R. Ohyama, T. Kobayashi, M. Suzuki, and K. Maruyama, Grain-boundary sliding in AZ31 magnesium alloys at room temperature to 523 K, *Mater. Trans*., 44(2003), No. 4, p .445.

[6] E. Yukutake, J. Kaneko, and M. Sugamata, Anisotropy and non-uniformity in plastic behavior of AZ31 magnesium alloy plates, *Mater. Trans.*, 44(2003), No. 4, p. 452.

[7] K. Iwanaga, H. Tashiro, H. Okamoto, and K. Shimizu, Improvement of formability from room temperature to warm temperature in AZ-31 magnesium alloy, *J. Mater. Process. Technol*., 155-156(2004), p. 1313.

[8] D.G. Kim, H.T. Son, D.W. Kim, Y.H. Kim, and K.M. Lee, The effect of texture and strain conditions on formability of cross-roll rolled AZ31 alloy, *J. Alloys Compd*., 509(2011), No. 39, p. 9413.

[9] L.L. Chang, E.F. Shang, Y.N. Wang, X. Zhao, and M. Qi, Texture and microstructure evolution in cold rolled AZ31 magnesium alloy, *Mater. Charact*, 60(2009), No. 6, p. 487.

[10] S.K. Mishra, S.M. Tiwari, J.T. Carter, and A. Tewari, Texture evolution during annealing of AZ31 Mg alloy rolled sheet and its effect on ductility, *Mater. Sci. Eng. A*, 599(2014), p. 1.

[11] Z. Xu, G. Tang, F. Ding, S. Tian, and H. Tian, The effect of multiple pulse treatment on the recrystallization behavior of Mg–3Al–1Zn alloy strip, *Appl. Phys. A*, 88(2007), No. 2, p. 429.

[12] X.N. Du, S.M. Yin, S.C. Liu, B.Q. Wang, and J.D. Guo, Effect of the electropulsing on mechanical properties and microstructure of an ECAPed AZ31 Mg alloy, *J. Mater. Res*., 23(2008), No. 6, p. 1570.

[13] L. Guan, G.Y. Tang, Y.B. Jiang, and P.K. Chu, Texture evolution in cold-rolled AZ31 magnesium alloy during electropulsing treatment, *J. Alloys Compd*., 487(2009), No. 1-2, p. 309.

[14] Y.B. Jiang, G.Y. Tang, C.H. Shek, and W. Liu, Microstructure and texture evolution of the cold-rolled AZ91 magnesium alloy strip under electropulsing treatment, *J. Alloys Compd*., 509(2011), No. 11, p. 4308.

[15] Y.B. Jiang, L. Guan, G.Y. Tang, C.H. Shek, and Z.H. Zhang, Influence of electropulsing treatment on microstructure and mechanical properties of cold-rolled Mg–9Al–1Zn alloy strip, *Mater. Sci. Eng. A*, 528(2011), No. 16-17, p. 5627.

[16] Y.B. Jiang, G.Y. Tang, C.H. Shek, J.X. Xie, Z.H. Xu, and Z.H. Zhang, Mechanism of electropulsing induced recrystallization in a cold-rolled Mg–9Al–1Zn alloy, *J. Alloys Compd*., 536(2012), p. 94.

[17] J.A. del Valle, M.T. Pérez-Prado, and O.A. Ruano, Texture evolution during large-strain hot rolling of the Mg AZ61 alloy, *Mater. Sci. Eng. A*, 355(2003), No. 1-2, p. 68.

[18] R.Z. Valiev, R.K. Islamgaliev, and I.V. Alexandrov, Bulk nanostructured materials from severe plastic deformation, *Prog. Mater. Sci*., 45(2000), No. 2, p. 103.

[19] S.R. Agnew and Ö. Duygulu, Plastic anisotropy and the role of non-basal slip in magnesium alloy AZ31B, *Int. J. Plast*., 21(2005), No. 6, p. 1161.

[20] Z.H. Xu, G.Y. Tang, S.Q. Tian, F. Ding, and H.Y. Tian, Research of electroplastic rolling of AZ31 Mg alloy strip, *J. Mater. Process. Technol*., 182(2007), No. 1-3, p. 128.